Microencapsulated G3C Hybridoma Cell Graft Delays the Onset of Spontaneous Diabetes in NOD Mice by an Expansion of Gitr$^+$ Treg Cells

Luigi Cari,[1] Pia Montanucci,[2] Giuseppe Basta,[2] Maria G. Petrillo,[1] Erika Ricci,[1] Teresa Pescara,[2] Alessia Greco,[2] Sabrina Cipriani,[3] Jun Shimizu,[4] Graziella Migliorati,[1] Giuseppe Nocentini,[1] Riccardo Calafiore,[2] and Carlo Riccardi[1]

Diabetes 2020;69:965–980 | https://doi.org/10.2337/db19-0087

As an alternative to lifelong insulin supplementation, potentiation of immune tolerance in patients with type 1 diabetes could prevent the autoimmune destruction of pancreatic islet β-cells. This study was aimed to assess whether the G3c monoclonal antibody (mAb), which triggers the glucocorticoid-induced TNFR-related (Gitr) costimulatory receptor, promotes the expansion of regulatory T cells (Tregs) in SV129 (wild-type) and diabetic-prone NOD mice. The delivery of the G3c mAb via G3C hybridoma cells enveloped in alginate-based microcapsules (G3C/cps) for 3 weeks induced Foxp3$^+$ Treg-cell expansion in the spleen of wild-type mice but not in Gitr$^{-/-}$ mice. G3C/cps also induced the expansion of nonconventional Cd4$^+$Cd25$^{-/low}$Foxp3^{low}Gitr$^{int/high}$ (GITR single-positive [sp]) Tregs. Both Cd4$^+$Cd25$^+$Gitr^{high}Foxp3$^+$ and GITRsp Tregs (including also antigen-specific cells) were expanded in the spleen and pancreas of G3C/cps-treated NOD mice, and the number of intact islets was higher in G3C/cps-treated than in empty cps-treated and untreated animals. Consequently, all but two G3C/cps-treated mice did not develop diabetes and all but one survived until the end of the 24-week study. In conclusion, long-term Gitr triggering induces Treg expansion, thereby delaying/preventing diabetes development in NOD mice. This therapeutic approach may have promising clinical potential for the treatment of inflammatory and autoimmune diseases.

Type 1 diabetes (T1D) is an autoimmune disease that is caused by the selective killing of pancreatic islet β-cells, which results in the shutdown of insulin production. Presently, lifelong exogenous insulin replacement is the only available therapy for these patients (1). More than 10 million people suffer from T1D worldwide, and disease-related complications impose a heavy burden on society (2). The inflammatory process and immune response are key factors in the development of T1D (3). In particular, autoreactive T cells and islet cell-reactive B lymphocytes play an important role in the development of this disorder (4,5). It has been reported that insulin-secreting cells can fully recover under conditions that restrain their destruction; this has led to the exploration of immunomodulatory approaches for T1D therapy (6–12). One of the first approaches used was immune cell depletion to prevent insulin-producing β-cells from being attacked and destroyed. However, this attempt did not meet with much success (13). Therefore, there is a clear need for alternative immunomodulatory methods that restrain pancreatic islet destruction in T1D.

Emerging evidence indicates that pancreatic resident regulatory T (Treg) cells exert immunosuppressive and anti-inflammatory effects, thereby suppressing overexuberant immune responses in T1D. Thus, an effective treatment for patients with T1D may involve the potentiation of

[1]Section of Pharmacology, Department of Medicine, University of Perugia, Perugia, Italy
[2]Section of Internal Medicine and Endocrine and Metabolic Sciences, Department of Medicine, and Laboratory for Endocrine Cell Transplants and Biohybrid Organs, University of Perugia, Perugia, Italy
[3]Rheumatology Unit, Department of Medicine, School of Medicine, University of Perugia, Perugia, Italy
[4]Center for Innovation in Immunoregulative Technology and Therapeutics, Graduate School of Medicine, Kyoto University, Kyoto, Japan
Corresponding author: Giuseppe Nocentini, giuseppe.nocentini@unipg.it

Received 25 January 2019 and accepted 25 February 2020

This article contains Supplementary Data online at https://diabetes.diabetesjournals.org/lookup/suppl/doi:10.2337/db19-0087/-/DC1.

L.C. and P.M. contributed equally to this study.

M.G.P. is currently affiliated with the Signal Transduction Laboratory, National Institute of Environmental Health Sciences, National Institutes of Health, U.S. Department of Health and Human Services, Research Triangle Park, Durham, NC.

immune tolerance via increasing the number of Treg cells (14). Indeed, engineered Treg cells expressing islet-specific antigens have shown good efficacy in T1D preclinical models (15–17). Thus, agents that can induce Treg-cell expansion should be explored further for their potential therapeutic benefits in T1D.

Glucocorticoid-induced TNFR-related (Gitr) protein, also known as TNFRSF18, is mainly expressed by T cells and plays a role in immune system homeostasis and immune-related disorders such as autoimmune diseases and cancer progression (18). A large number of Treg cells express high levels of Gitr in the microenvironment of human cancers (19,20), and Gitr expression is correlated with more aggressive cancer and worse prognosis (21,22). Therefore, Gitr is one of the activated Treg-cell markers that are crucial in determining the suppressive microenvironment of tumors. Indeed, some Gitr-triggering reagents promote tumor rejection by inducing antibody-dependent cellular cytotoxicity (ADCC) of Treg cells (23,24).

Transfer of Gitr-depleted T cells into BALB/c nude mice results in the death of 90% of the mice due to autoimmune disease development, thus indicating that $Gitr^+$ cells play a crucial role in immune homeostasis (25). Furthermore, in systemic lupus erythematosus and Sjögren syndrome, the expansion of $Cd4^+Cd25^{-/low}Foxp3^{low}Gitr^{int/high}$ (GITR single-positive [sp]) Treg cells was found in patients with low disease activity, thus confirming that $Gitr^+$ cells play a role in immune homeostasis in humans too (26,27).

Gitr is a costimulatory receptor, and its triggering favors the activation and expansion of T cells, including conventional $Cd4^+$ T cells, effector $Cd8^+$ T cells, and Treg cells (18). The resulting in vivo effects depend on the context, the type of disease, and the way by which Gitr is stimulated (28). Despite the context-dependent effect of Gitr triggering, we can assume that the main effects of Gitr triggering favor the expansion of Treg cells based on the reported evidence (19). For example, the number of Treg cells is lower in mice knockout for Gitr and Gitr ligand (GitrL) (29–31) and higher in GitrL transgenic mice (32,33). Moreover, some anti-Gitr monoclonal antibodies (mAbs; e.g., G3c mAb) and GitrL fusion proteins do not promote tumor rejection because they stimulate Treg-cell expansion without promoting ADCC (34,35). In the context of T1D, this could mean that treatment with anti-Gitr mAbs may favor a $Gitr^+$ Treg-cell expansion, which prevents β-cell destruction by locally restraining inflammatory responses. To explore this possibility, in the current study, we treated diabetes-prone NOD mice with the anti-Gitr G3c mAb and explored its potential antidiabetic effects, with promising results.

RESEARCH DESIGN AND METHODS

Culture of G3C Hybridoma Cells Culture and Preparation of G3c-Secreting Microcapsules

G3C hybridoma cells were cultured in RPMI medium (Gibco) with 10% FBS. When purification of IgM mAbs was needed (ELISA standard curve), cells were cultured in CD Hybridoma serum-free chemical medium (CD Hybridoma Medium, supplemented with 250× Cholesterol Lipid Concentrate) (Gibco). To fabricate G3c-secreting microcapsules that would allow for the outflow of big molecules (such as an IgM), we had to modify the standard microencapsulation procedure; we changed stoichiometric molar ratios of ultrapurified alginate (AG) and poly-L-ornithine, used for microencapsulation. We also changed the composition of the capsule's multilayered membrane, by reframing the layering sequence to fulfill the desired membrane's molecular weight cutoff. The functionality test and the details on the preparation of the G3c-secreting microcapsules have been provided elsewhere (36). We used 1.5×10^6 G3C hybridoma cells/1 mL AG; such an AG-to-cell ratio would avoid the formation of empty capsules.

Purification of G3c mAb and ELISA

G3C hybridoma cells were cultured for 14 days in a serum-free chemical medium (CD Hybridoma Medium, supplemented with 250× Cholesterol Lipid Concentrate) (Gibco). G3c-derived mAb was purified using HiTrap IgM Purification HP column (1 mL size) for affinity purification (GE Healthcare) following the manufacturer's instructions. The buffer containing purified G3c mAb was exchanged with PBS through dialysis by using the Slide-A-Lyzer Dialysis Cassette (10,000 molecular weight cut-off) (Thermo Fisher Scientific). The purified G3c mAb was quantified using the Bradford method. We developed an ELISA to quantify the level of G3c mAb produced by G3C cells, as described elsewhere (36).

For the quantization of Igs in the serum of SV129 and $Gitr^{-/-}$ mice, we used commercially available kits following the manufacturer's instructions (Mouse Uncoated ELISA kits for IgG1 [cat. 88-50410-22], IgG2a [cat. 88-50420-22], IgG2b [cat. 88-50430-22], IgG2c [cat. 88-50670-22], and IgG3 [cat. 88-50440-22]; all kits were purchased from Thermo Fisher Scientific).

Animals and Grafts

NOD mice were purchased from The Jackson Laboratory (Bar Harbor, ME). Female SV129 and $Gitr^{-/-}$ SV129 mice were available in our laboratory. The animals were housed in a controlled environment, provided with standard rodent chow and water ad libitum, and kept under specific pathogen-free conditions. Animal care complied with regulations in Italy (D.M. 116192), Europe (O.J. of E.C. L 358/1 12/18/1986), and the U.S. (Animal Welfare Assurance No. A5594–01). The encapsulated G3C hybridoma cells were grafted intraperitoneally into mice under general anesthesia. For each mouse, 1.5×10^6 G3C hybridoma cells in 1 mL of microcapsules (G3C/cps) or 1 mL of empty microcapsules (e/cps) as a control, were grafted. All procedures were approved by the University of Perugia Committee of Animal Research and Ethics.

Study Design of In Vivo Experiments

SV129 and $Gitr^{-/-}$ SV129 mice (11 weeks old) were grafted with e/cps ($n = 5$ wild type [WT] and $n = 5$ $Gitr^{-/-}$ mice)

and G3C/cps ($n = 6$ WT and $n = 6$ Gitr$^{-/-}$ mice) and sacrificed 3 weeks after. Five WT and five Gitr$^{-/-}$ untreated mice (14 weeks old) were used as control groups. The protocol is summarized in Supplementary Fig. 1.

In the short-term experiment, NOD mice (8 weeks old) were grafted with e/cps ($n = 8$ mice) and G3C/cps ($n = 8$ mice) and sacrificed 3 weeks after. Four mice (8 weeks old at baseline) were used as the control group. The protocol is summarized in Supplementary Fig. 1.

In the long-term experiment, NOD mice (11 weeks old) were grafted with e/cps ($n = 24$ mice) and G3C/cps ($n = 22$ mice) and sacrificed 3 months after (when they were 24 weeks old) or when they had a persistent high blood glucose (BG) level (2 BG >500 mg/dL). Control groups comprised *1*) the baseline control group ($n = 4$ mice sacrificed when they were 11 weeks old) and *2*) the untreated control group ($n = 10$ mice, 11 weeks old) that were left untreated and sacrificed when 24 weeks old or when they had a persistent high BG level. The protocol is summarized in Supplementary Fig. 1.

During the long-term experiment, one e/cps-treated NOD mouse and one G3C/cps-treated NOD mouse showed weight loss, severe hypoglycemia, and salivary gland abscess, and they were sacrificed. These mice were not considered in the long-term experiment.

Morphological Evaluations of the Pancreas

After the sacrifice of the NOD mice, histological evaluation of the pancreas was performed using a score adapted from one previously described (37). Briefly, 3–4 μm of paraffin-embedded sections from half of the pancreas were used to prepare 24 slides. Then, 5 among 15 consecutive histological sections were placed on each slide, and among the 24 slides, 8 slides were stained with hematoxylin and eosin by skipping 2 of 3 consecutive slides. Only one of five sections on the slide was analyzed by light microscopy and scored. Insulitis scoring was defined according to the following criteria: *1*) intact without insulitis, an islet that shows absence of cell infiltration; *2*) intact with insulitis, an islet that is damaged (<50% of the islet area infiltrated or infiltration is restricted to the periphery of the islet); or *3*) disrupted, an islet with severe intrainsulitis in which >50% of the islet area is infiltrated.

In the short-term experiment, 591 islets were scored (a mean of 27.6 ± 6.6 islets for baseline mice, 24.7 ± 8.6 islets for e/cps-treated mice, and 22.0 ± 6.9 islets for G3C/cps-treated mice). In the long-term experiment, 986 islets were scored (a mean of 20.8 ± 9.3 islets for baseline mice, 18.3 ± 11.3 islets for untreated control mice, 16.7 ± 13.3 islets for e/cps-treated mice, and 18.5 ± 10.8 islets for G3C/cps-treated mice).

NOD BG Evaluations

BG levels in NOD mice were evaluated twice weekly by blood sampling from the tail of the animals and measurement of glucose levels with a standard BG meter (37).

Flow Cytometry

Cells from the spleen, pancreas, and pancreatic lymph nodes were recovered as previously described (37).

All cytofluorimetric evaluations were performed on the Attune NxT Flow Cytometer system (Thermo Fisher Scientific) using fluorochrome-conjugated monoclonal antibodies against B220 (clone RA3-6B2), Cd3 (clone 145-2C11), Cd4 (clone GK1.5), Cd8 (clone 53-6.7), Foxp3 (clone FJK-16s), Gitr (clone DTA-1), Cd25 (clone PC61.5), Cd44 (clone IM7), and CD62L (clone MEL-14). All antibodies were provided by Thermo Fisher Scientific. Before Foxp3 staining, cells were permeabilized with the Foxp3/Transcription Factor Staining Buffer Set (Thermo Fisher Scientific) following the manufacturer's instructions.

For cell proliferation studies, cells were labeled with the CellTrace Violet Cell Proliferation Kit for flow cytometry (Thermo Fisher Scientific) following the manufacturer's instructions. After staining, cells were cultivated for 3 days in the presence of anti-Cd3 (1:500, functional grade, clone OKT3) (Thermo Fisher Scientific) and anti-CD28 (1:5,000, functional grade, clone 37.51) (Thermo Fisher Scientific) cross-linked to U-shaped wells (96-well plate). Before flow cytometry evaluation, splenocytes were stained with fluorochrome-conjugated anti-B220, -Cd3, -Cd4, and -Cd8 antibodies, and the proliferation rate of CellTrace Violet-labeled B220$^-$Cd3$^+$Cd8$^-$Cd4$^+$ cells was evaluated.

For the evaluation of the antigen-specificity of Treg-cell populations, we stained cells with fluorochrome-conjugated tetramers following the manufacturer's instructions (IGRP Tetramer-VYLKTNVFL-APC, cat. TB-M552-2; NRP Tetramer-KYNKANVFL-BV421, cat. TB-M553-4; and InsB Tetramer-LYLVCGERL-PE, cat. TS-M554–1; all tetramers were purchased from MBL International). To evaluate the antigen-specificity of Treg-cell populations, splenocytes or cells from the pancreas and pancreatic lymph nodes were stained with fluorochrome-conjugated tetramers together with fluorochrome-conjugated anti-B220, -Cd3, -Cd4, -Cd8, -Gitr, and -Cd25 antibodies. Isolation of immune cells from the pancreas and pancreatic lymph nodes resulted in a relatively low number of cells, so that the events detected in the B220$^-$Cd3$^+$Cd8$^-$CD4$^+$ gate when tetramers and antibodies against surface markers were stained ranged between 1,500 and 10,000 events, considered to be sufficient for analysis. When intracellular staining of Foxp3 cells was performed, two samples were excluded due to the above reason. In not excluded samples, the mean events in B220$^-$Cd3$^+$Cd8$^-$CD4$^+$ gate were equal to 1,596.

Real-time Quantitative PCR

Total RNA from the pancreas of NOD mice was isolated using Trizol reagent (Thermo Fisher Scientific), and the generation of cDNA was performed using a PrimeScript RT Reagent Kit (Takara Bio Europe). Real-time quantitative (q)PCR was done with an ABI-7300 Real-time PCR system (Applied Biosystems) using specific FAM/MGB dye-labeled TaqMan probes (Mm00442754_m1 for Cd4,

Mm01182107_g1 for Cd8, Mm00475162_m1 for Foxp3, Mm00437136_m1 for Gitr, and Mm01340213_m1 for Cd25). Gene expression was quantitated relatively to the expression of endogenous control GAPDH (4352339E) VIC/MGB probe amplified in the same tube of the investigated genes. All probes were purchased from Applied Biosystems (Thermo Fisher Scientific). All experiments were repeated twice, and the $\Delta\Delta$ threshold cycle method was used to determine the expression of the genes of interest, as previously described (38).

Statistical Analysis

Kolmogorov-Smirnov (KS) normality test was performed on data from each group before statistical evaluation. To evaluate the differences between groups, *P* values were calculated using ordinary one-way ANOVA (Tukey) test when the KS normality test was passed and Kruskal-Wallis (Dunn) test when KS normality test failed. In the evaluation of the percentage of diabetic mice in the long-term experiment, the Fisher exact contingency test was performed. In the evaluation of the posttreatment day at which mice developed diabetes, the unpaired Student *t* test was performed. The log-rank Mantel-Cox test was used to compare Kaplan-Meier curves. The hazard ratio (95% CI) was calculated using the Mantel-Haenszel method. All statistical analyses were conducted using Prism software (GraphPad Software).

Data and Resource Availability

No data sets were generated or analyzed during the current study. The hybridoma G3C that supports the findings of this study is available from Kyoto University Medical Science and Business Liaison Organization, but restrictions apply to the availability of this cell line, which was used under license for the current study and therefore is not publicly available. The hybridoma G3C may be available from the authors and/or Kyoto University Medical Science and Business Liaison Organization upon reasonable request and with permission of Kyoto University Medical Science and Business Liaison Organization.

RESULTS

G3c mAb Induces the Expansion of Conventional and Nonconventional Treg Cells in WT Mice but Not in Gitr$^{-/-}$ Mice

To administer high-quality fully active antibodies, we encapsulated the G3C hybridoma cells in AG-based microcapsules. Microcapsules have been previously used by other groups and by us to deliver cell-derived products in vivo (39–41). The microcapsules used in this study were modified so that the G3c mAb (an IgM-type antibody) could exit the capsule. The microencapsulated hybridoma cells survived for several days in the in vitro culture and for several weeks when transferred into the peritoneum of mice. Details about how the capsules were manufactured, their properties, and IgM delivery are reported elsewhere (36).

We grafted empty microcapsules (e/cps) or the G3C-containing microcapsules (G3C/cps) in the peritoneum of WT and Gitr$^{-/-}$ mice. Mice were euthanized 3 weeks after microcapsule implantation (Supplementary Fig. 1). Notably, the microcapsules did not elicit an inflammatory response (36), and a detectable amount of the G3c mAb was found in the blood of the mice (Supplementary Fig. 2). However, serum concentrations of the G3c mAb were higher in Gitr$^{-/-}$ than in WT mice, probably due to the target-dependent peripheral distribution of the G3c mAb in WT mice.

Then, we investigated the effects of both surgical procedure and treatment by evaluating the main cellular (Supplementary Fig. 3) and humoral immunity (Supplementary Fig. 4) features. G3c treatment showed some effects on the immune system of both WT and Gitr$^{-/-}$ mice, as demonstrated by the increase of spleen weight and the number of splenocytes and B lymphocytes in the spleen. Furthermore, the number of splenic Cd3$^+$ and Cd4$^+$ T lymphocytes showed a significant increase in WT but not in Gitr$^{-/-}$ mice after the treatment. Conversely, G3c treatment did not affect the number of Cd8$^+$ T splenocytes. Thus, the antibody has some aspecific actions on both WT and Gitr$^{-/-}$ mice and specific effects (reasonably mediated by Gitr triggering) in WT mice concerning the number of Cd4$^+$ cells and, consequently, Cd3$^+$ cells.

G3c inoculation affected also humoral immunity. IgG3 and IgG2c increased in both WT and Gitr$^{-/-}$ mice after G3c treatment; meanwhile, IgG2a significantly increased in G3C/cps-treated compared with e/cps-treated only in WT mice, and the increase was relevant (approximately threefold). The increase of Cd3$^+$ T cells, Cd4$^+$ T cells, and IgG2a in G3C/cps-treated WT animals may suggest that the effect of G3C treatment is restricted to a specific immune response that promotes an immune-activating effect.

Based on the known expression and effects of Gitr on Treg cells, we investigated whether the number of splenic Foxp3$^+$ Treg cells changed in response to G3c treatment. As shown in Fig. 1*A*, the number of splenic Foxp3$^+$ Treg cells was higher in G3C/cps-treated than in untreated WT mice, but no difference was observed between treated and untreated Gitr$^{-/-}$ mice. Thus, the increase in the number of Foxp3$^+$ Treg cells in the G3C/cps-treated WT mice may depend on Gitr triggering. This is supported by the finding that Gitr levels were higher in Foxp3$^+$ Treg than in conventional T splenocytes (Fig. 1*B*). In addition, the number of Foxp3$^+$Cd25$^+$Gitr^{high} Treg cells is higher in G3C/cps-treated mice compared with e/cps-treated and untreated mice (Fig. 1*C*).

We recently demonstrated the existence of GITRsp cells in humans (42,43), their regulatory activity, and their suppressive role in systemic lupus erythematosus and Sjögren syndrome (26,27). Murine GITRsp unconventional Tregs are Foxp3$^{-/low}$ and Cd25$^{-/low}$ (Supplementary Fig. 5). Here, we found that after in vivo treatment with G3c mAb, the number of GITRsp cells was more than twice the number in G3C/cps-treated WT mice compared with

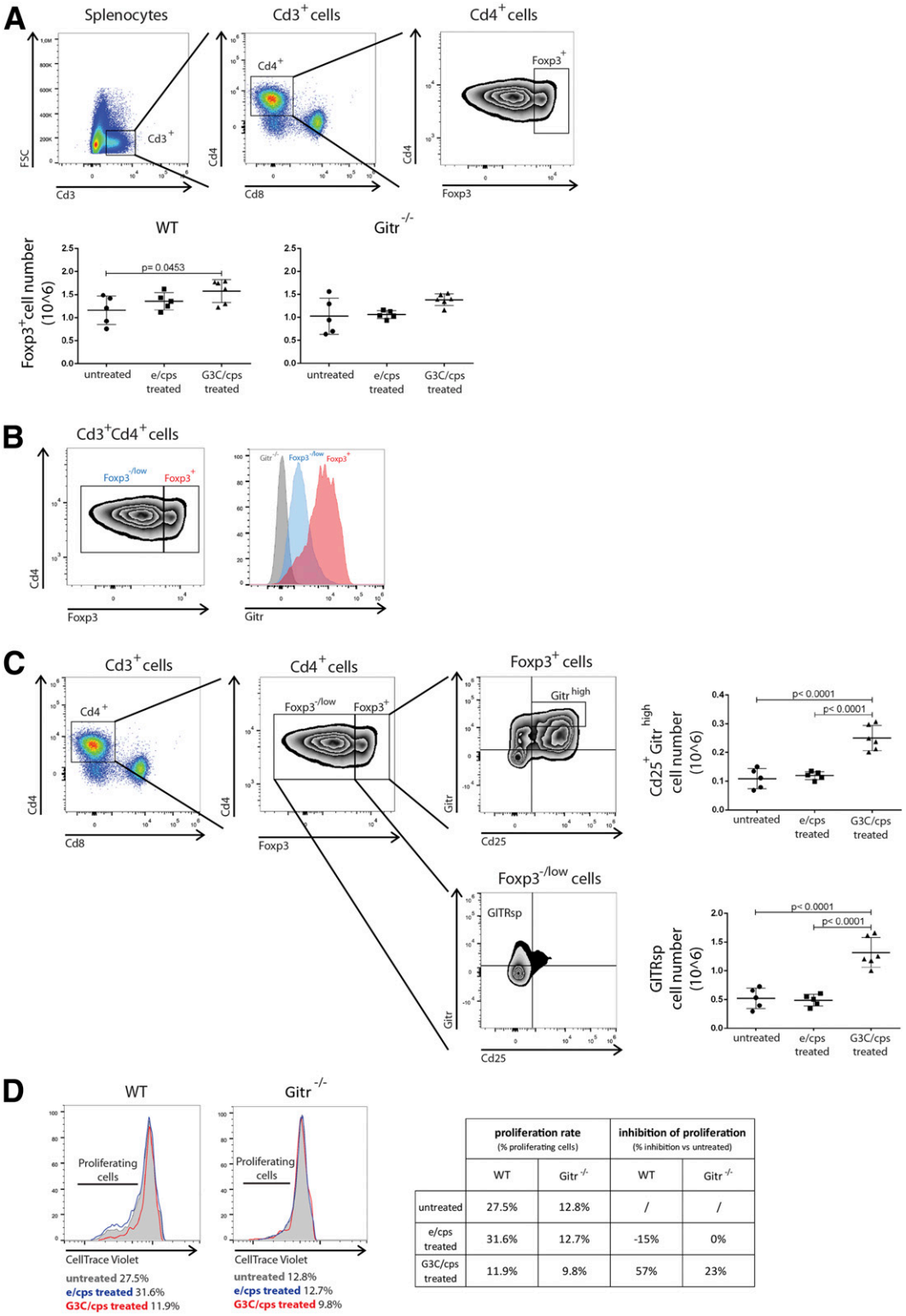

	proliferation rate (% proliferating cells)		inhibition of proliferation (% inhibition vs untreated)	
	WT	Gitr -/-	WT	Gitr -/-
untreated	27.5%	12.8%	/	/
e/cps treated	31.6%	12.7%	-15%	0%
G3C/cps treated	11.9%	9.8%	57%	23%

Figure 1—G3c-dependent expansion of conventional and nonconventional Treg subsets in the spleens of WT mice but not in the spleens of Gitr$^{-/-}$ mice. *A*: Cd3^{+}Cd4^{+}Foxp3^{+} splenocytes of WT (lower left panel) and Gitr$^{-/-}$ (lower right panel) mice that were left untreated or treated with e/cps or G3C/cps. The dot plots and zebra plot (upper panels) represent the gating strategy. *B*: Gitr is more expressed in Cd3^{+}Cd4^{+}Foxp3^{+} cells than in Cd3^{+}Cd4^{+}Foxp3$^{-/low}$ cells. The zebra plot on the left represents the gating strategy for the Cd3^{+}Cd4^{+} splenocytes. The histogram on the right depicts the expression of Gitr on Cd3^{+}Cd4^{+}Foxp3$^{-/low}$ and Cd3^{+}Cd4^{+}Foxp3^{+} splenocytes from WT mice. As a control, the expression of Gitr on Cd3^{+}Cd4^{+} splenocytes from Gitr$^{-/-}$ mice is shown. A representative staining is shown. *C*: Cd3^{+}Cd4^{+}Foxp3^{+}Cd25^{+}Gitr^{high} cell number (upper right panel) and Cd3^{+}Cd4^{+}Foxp3$^{-/low}$Cd25^{-}Gitr$^{int/high}$ (GITRsp) cell number (lower right

e/cps-treated and untreated WT mice (Fig. 1*C*). Furthermore, the proliferation rate of conventional $Cd4^+$ T splenocytes isolated from G3C/cps-treated WT mice was lower than in $Cd4^+$ cells isolated from untreated and e/cps-treated WT mice (Fig. 1*D*). On the contrary, the proliferation rate of $Cd4^+$ conventional T splenocytes from untreated, e/cps-treated, and G3C/cps-treated $Gitr^{-/-}$ mice showed no substantial difference, thus indicating that the expanded $Foxp3^+Cd25^+Gitr^{high}$ and GITRsp Treg cells were fully active.

Taken together, these results indicate that G3c mAb induces conventional and nonconventional Treg-cell expansion via Gitr triggering.

Gitr Triggering by G3c mAb Induces the Expansion of Conventional and Nonconventional Treg Cells in NOD Mice and Protects Pancreatic Islets From Damage

We grafted G3C/cps and e/cps into the peritoneum of nondiabetic NOD mice (Supplementary Fig. 1) and evaluated the number of immune cells in the spleen at 3 weeks after the implant.

Similar to SV129 mice, also in NOD mice, G3c mAb had some effects on the growth of splenocytes, B cells, and T cells (Supplementary Fig. 6). Moreover, not only the number of $Cd4^+$ but also of $Cd8^+$ cells was increased.

As seen in SV129 mice, the percentages and the absolute numbers of splenic $Foxp3^+$ and $Foxp3^+Cd25^+Gitr^{high}$ increased after G3c treatment, and the increase was at least partly due to the increase of $Gitr^{high}$ cells (Fig. 2*A* and *B*). Similarly, nonconventional GITRsp Treg cells were higher in the spleen of G3C/cps-treated NOD mice than in the spleen of untreated and e/cps-treated NOD mice (Fig. 2*A* and *B*). The surgical procedure and treatment with e/cps had some effects on the percentage but not in the absolute number of cell subsets. In any case, the effects were less relevant than G3C/cps treatment.

Interestingly, we found a higher number of memory T cells in $Foxp3^+Cd25^+Gitr^{high}$ cells than in $Foxp3^+Cd25^+Gitr^{-/low}$ cells and in GITRsp cells than in $Foxp3^-Cd25^-Gitr^{-/low}$ T cells (Supplementary Fig. 7). This suggests that the expanded conventional and nonconventional $Gitr^+$ Treg cells might be antigen-specific cells. We therefore evaluated the percentage of GITRsp and $Cd25^+Gitr^{high}$ cells recognizing three antigens—Igrp, Nrp, and Insb—considered to be implied in T1D development. Results shown in Fig. 2*C* show that the percentages of $tetramer^+Cd25^+Gitr^{high}$ and $tetramer^+$GITRsp cells in the spleen of NOD mice were higher after treatment compared with untreated mice as concerns $Igrp^+$ and $Insb^+$ cells (~1.5 fold). The increase was observed in e/cps- and in G3C/cps-treated mice, although the increase of $tetramer^+Cd25^+Gitr^{high}$ was higher in G3C/cps-treated than in e/cps-treated mice. Moreover, the increase of the percentage of antigen-specific subpopulations within the GITRsp and $Cd25^+Gitr^{high}$ cells was not observed (Supplementary Fig. 8), suggesting that the increase of T1D-related antigen-specific cell subpopulations was similar to the increase of other antigen-specific cells that may or may not be restricted to T1D-inducing antigens.

We next evaluated the presence of Tregs in the pancreatic lymph nodes and pancreatic immune infiltrate at 3 weeks after the implantation. The data we obtained were similar to the data found in splenocytes but more relevant from a quantitative point of view (Fig. 3*A*). Interestingly, we observed no effect on the percentages of $Foxp3^+$, $Foxp3^+Cd25^+Gitr^{high}$, and GITRsp Treg cells in e/cps mice, suggesting that the increase of the above-specified subpopulations in the pancreas is exclusively due to Gitr triggering.

The percentage of Igrp-, Nrp-, and Insb-specific Treg cells in the pancreatic lymph nodes and the pancreatic immune infiltrate at 3 weeks after the implantation was substantially increased compared with untreated NOD mice and/or e/cps-treated mice (Fig. 3*B*). The only exception was Igrp-specific GITRsp cells. Interestingly, Insb-specific $Cd25^+Gitr^{high}$ and GITRsp cells showed a relevant increase after only G3C/cps treatment (6- to 11-fold compared with the untreated animals). Of note, Insb-specific subpopulations increased within the GITRsp cells (Supplementary Fig. 9), suggesting that the increase of these subpopulations was driven by antigen-specific cells. The increase of $Insb^+Cd25^+Gitr^{high}$ was similar to that of $Insb^+$ GITRsp cells, even if not significant.

Furthermore, we evaluated the effects of G3c treatment on pancreas histology. Pancreatic islets were divided into three groups according to their histological appearance (Fig. 3*C*): intact without insulitis (an islet that shows absence of cell infiltration), intact with insulitis (an islet that is damaged in which <50% of the islet area is infiltrated or infiltration is restricted to the periphery of the islet), or disrupted (an islet with severe intrainsulitis in which >50% of the islet area is infiltrated). As shown in Fig. 3*C*, the percentage of islets that were intact without insulitis and disrupted was different between the pancreas of G3C/cps- and e/cps-treated NOD mice. In both cases, the pancreas from G3C/cps-treated NOD mice showed comparable values to untreated 8-week-old mice (baseline mice).

panel) from the spleen of mice that were left untreated or treated with e/cps or G3C/cps. The dot plot and zebra plots on the left represent the gating strategy. *D*: Splenocytes of WT (left panel) and $Gitr^{-/-}$ (right panel) mice that were left untreated or treated with e/cps or G3C/cps were activated by cross-linked anti-Cd3 (1:500) and anti-Cd28 (1:5,000) antibodies. The proliferation rate of CellTrace Violet-stained $Cd4^+$ T cells was evaluated after 3-day activation. The inhibition of proliferation of cells of treated mice compared with untreated is reported in the table. The *P* values for *A* and *C* were calculated using one-way ANOVA (Tukey) or Kruskal-Wallis (Dunn) when the KS normality test failed. Nonsignificant values ($P > 0.05$) are not shown.

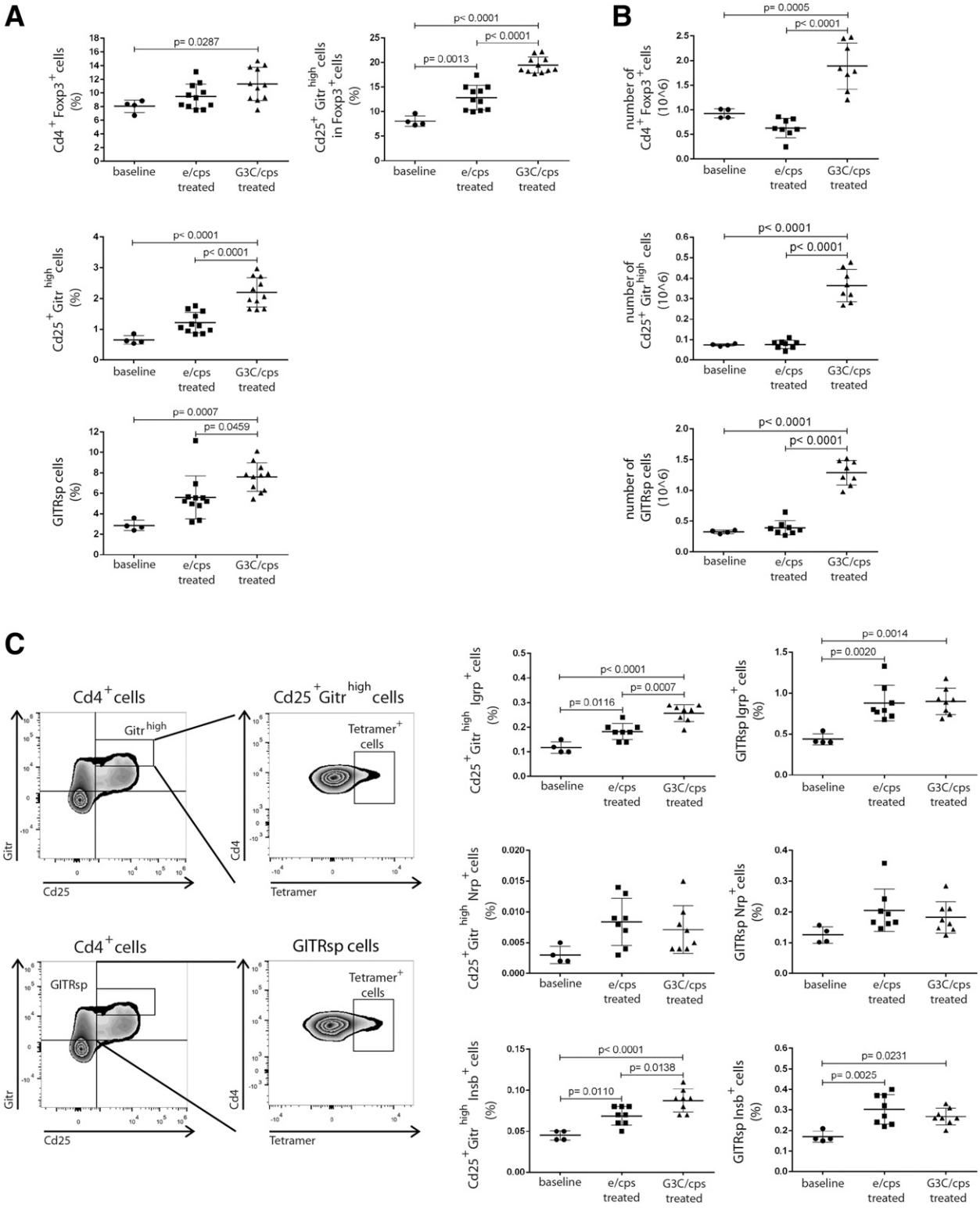

Figure 2—G3c-dependent expansion of conventional and nonconventional Treg-cell subsets in the spleen of NOD mice in the short-term experiment. *A*: Percentage of $Cd4^+Foxp3^+$ cells in $Cd3^+$ splenocytes (upper left panel), of $Cd25^+Gitr^{high}$ cells in $Cd4^+Foxp3^+$ splenocytes (upper right panel), of $Cd4^+Foxp3^+Cd25^+Gitr^{high}$ cells in $Cd3^+$ splenocytes (middle left panel), and of $Cd4^+Foxp3^{-/low}Cd25^-Gitr^{int/high}$ (GITRsp) cells in $Cd3^+$ splenocytes (lower left panel) from NOD mice, 3 weeks after the graft of e/cps or G3C/cps compared with the same cells of control mice (baseline). The gating strategy is identical to that reported in Fig. 1*C*. *B*: The number of $Cd3^+Cd4^+Foxp3^+$ splenocytes (upper panel), of $Cd3^+Cd4^+Foxp3^+Cd25^+Gitr^{high}$ splenocytes (middle panel), and of $Cd3^+Cd4^+Foxp3^{-/low}Cd25^-Gitr^{int/high}$ (GITRsp) splenocytes (lower panel) from NOD mice, 3 weeks after the graft of e/cps or G3C/cps compared with the same cells of control mice (baseline). The gating strategy is identical to that reported in Fig. 1*C*. *C*: Percentage of $Cd25^+Gitr^{high}Igrp^+$ (upper left graph), $Cd25^+Gitr^{high}Nrp^+$ (middle left graph), and $Cd25^+Gitr^{high}Insb^+$ cells (lower left graph) in $Cd3^+Cd4^+$ splenocytes, and percentage of $Igrp^+$

These findings indicate that Treg-cell expansion via Gitr triggering inhibits islet attack by the immune system during the development of diabetes.

Long-term G3c mAb Treatment Prevents/Delays Diabetes Development in NOD Mice

We implanted G3C/cps and e/cps in the peritoneum of nondiabetic NOD mice and evaluated the BG level for each untreated and cps-treated mouse every 48−72 h (Supplementary Fig. 1). Figure 4*A* shows that several untreated and e/cps-treated NOD mice developed diabetes since BG levels were higher than normal in at least two consecutive evaluations. However, in all except two G3C/cps-treated NOD mice, the BG level remained <200 mg/dL during the whole observation period, with the exception of sporadic, nonconsecutive evaluation; this means that the treatment delays diabetes development. Indeed, one G3C/cps-treated NOD mouse developed diabetes 77 days after the beginning of the treatment and another showed a BG of 300 mg/dL on day 89. Not having a second BG measurement, we could not assess the onset of diabetes in the latter mouse, but we considered this mouse diabetic. On the contrary, it was considered as alive in the Kaplan-Meyer survival curve, because unlike the others, it was not euthanized due to diabetes.

In conclusion, we found that G3C/cps-treated NOD mice had a higher survival rate than untreated and e/cps-treated NOD mice (Fig. 4*B*). These results suggest that G3c treatment prevents or delays the onset of diabetes in NOD mice.

Long-term G3c mAb Treatment Prevents the Destruction of Pancreatic Islets in NOD Mice

Figure 5*A* shows the percentage of islets that were "intact without insulitis" and "disrupted" differed between the pancreas of G3C/cps- and e/cps-treated NOD mice. A similar difference was observed between the pancreas of G3C/cps-treated and untreated NOD mice, but it resulted in a nonsignificant difference, presumably due to the lower number of studied mice. G3C/cps-treated NOD mice showed comparable values of "disrupted" islets to those of baseline, 11-week-old mice (13 weeks younger than G3C/cps-treated NOD mice). Figure 5*B* shows that the "disrupted"-to-"intact without insulitis" ratio was <1 in baseline young mice and G3C/cps-treated mice and >1 in untreated and e/cps-treated mice, likely indicating that the beneficial effects of the G3C/cps treatment is related to the protection of the islets from autoimmune attack.

When we compared the histology of the islets in mice that were nondiabetic at the end of the 90-day period (Fig. 5*A*, right panel), no significant differences were observed among G3C/cps-treated, untreated, and e/cps-treated mice, possibly suggesting that G3c treatment potentiates the immune homeostatic attempts that occur in NOD mice not developing the disease.

The Presence of Treg Cells in the Pancreas Protects Pancreatic Islets in G3c-Treated NOD Mice

To understand whether G3c treatment protects pancreatic islets from destruction through the same homeostatic mechanisms activated in NOD mice spontaneously remaining diabetes-free or through other mechanisms, we evaluated whether the effects observed at 3 weeks postmicrocapsule implantation were still observable after 3 months in G3c-treated mice and whether they were similar to untreated NOD mice remaining diabetes free.

First, we evaluated the splenocyte cell composition. Figure 6 shows that in all mice (left panels) and in nondiabetic mice (right panels), the three Treg subsets that underwent expansion 3 weeks after G3c treatment show a less relevant expansion compared with that observed after the 3-week treatment. In particular, $Cd25^+Gitr^{high}$ and GITRsp cells did not show significant expansion compared with e/cps-treated mice but showed significant expansion compared with untreated animals. On the contrary, the increase of $Cd25^+Gitr^{high}$ in $Foxp3^+$ cells is still present both in all and in nondiabetic mice.

Then, we evaluated the infiltration of $Cd4^+$, $Cd8^+$, and conventional and nonconventional Treg cells by real-time qPCR in nondiabetic and diabetic NOD mice that were implanted with empty and G3C microcapsules or left untreated. Figure 7*A* shows that similar levels of $Cd4^+$ and $Cd8^+$ T cells were present in the pancreas of all the animals, thus suggesting that the treatment does not affect T-cell infiltration. Independently from treatment, no differences were observed between diabetic and nondiabetic mice, implying that the development of diabetes was not dependent on the infiltration levels of $Cd8^+$ T cells.

Next, we evaluated the mRNA levels of Foxp3, Gitr, and Cd25. Figure 7*B* shows that the level of Foxp3 expression is much higher in G3c-treated mice than in the other groups and that all nondiabetic mice have Foxp3 values higher than diabetic mice. However, the significance is seen only between G3c-treated mice and diabetic mice (both untreated and e/cps-treated). A similar reasoning can be done observing Gitr expression but not Cd25 expression. The nonsignificant difference among the groups in the expression of Cd25 may be due to the expression of Cd25 even in activated T cells.

The findings may suggest that G3c treatment favors the infiltration of the pancreas and/or homing in pancreatic

(upper right graph), Nrp^+ (middle right graph), and $Insb^+$ (lower right graph) GITRsp cells in $Cd3^+Cd4^+$ splenocytes from NOD mice, 3 weeks after the graft of e/cps or G3C/cps compared with the same cells of control mice (baseline). The zebra plots (left panels) represent the gating strategy. The *P* values for *A*, *B*, and *C* were calculated using one-way ANOVA (Tukey) or Kruskal-Wallis (Dunn) when the KS normality test failed. Nonsignificant values ($P > 0.05$) are not shown.

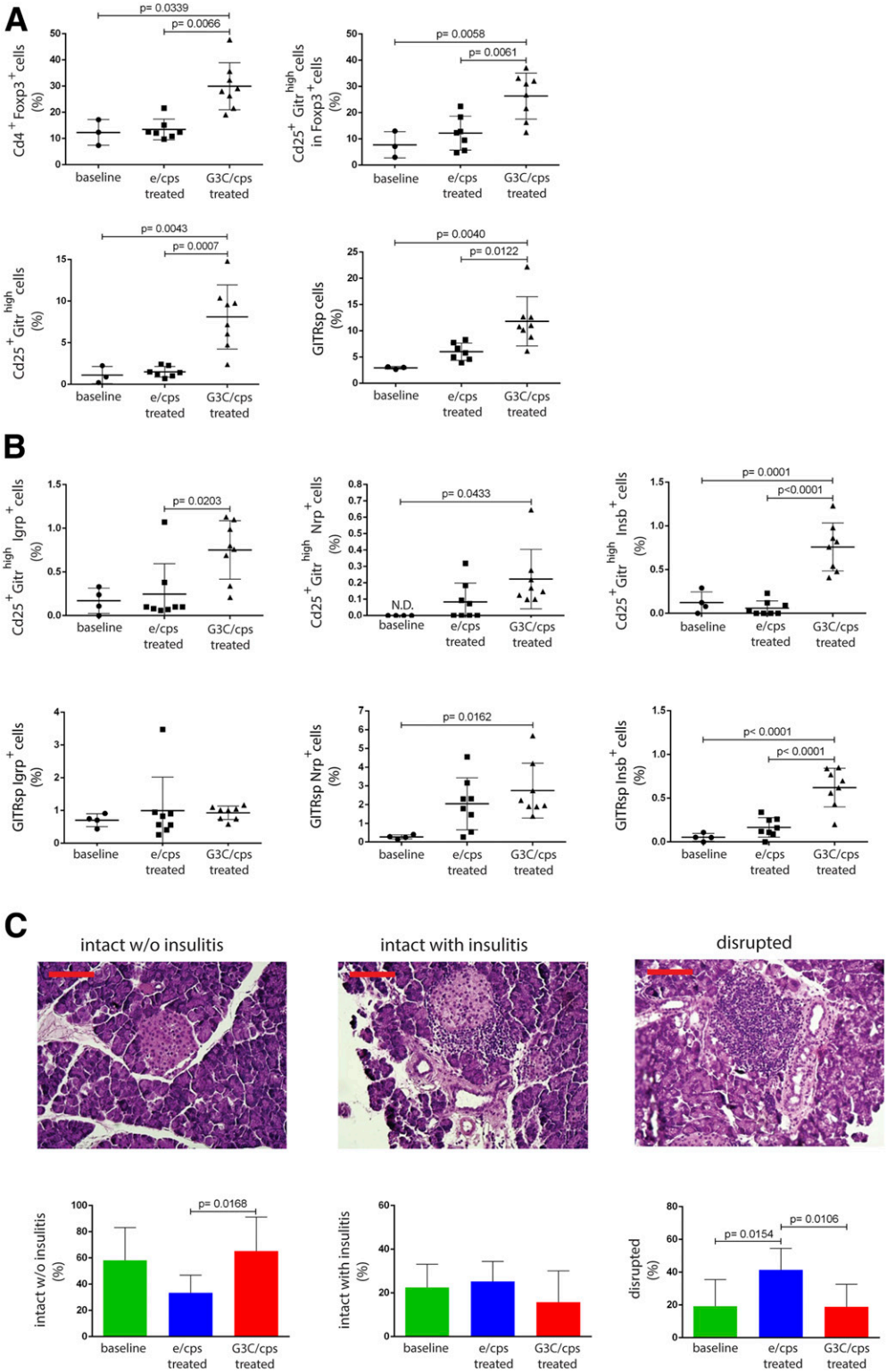

Figure 3— G3c-dependent expansion of conventional and nonconventional Treg subsets in the pancreas of NOD mice and their effect on pancreatic islet damage in the short-term experiment. *A*: Percentage of $Cd4^+Foxp3^+$ cells in $Cd3^+$ cells (upper left panel), $Cd4^+Foxp3^+Cd25^+Gitr^{high}$ cells in $Cd4^+Foxp3^+$ cells (upper right panel), $Cd4^+Foxp3^+Cd25^+Gitr^{high}$ cells in $Cd3^+$ cells (lower left panel), and $Cd4^+Foxp3^{-/low}Cd25^-Gitr^{int/high}$ (GITRsp) cells in $Cd3^+$ cells (lower right panel) isolated from pancreas infiltrate and pancreatic lymph nodes of NOD mice 3 weeks after the graft of e/cps or G3C/cps compared with the same cells of control mice (baseline). The gating strategy is identical to that reported in Fig. 1*C*. *B*: Percentage of $Cd25^+Gitr^{high}Igrp^+$ (upper left panel), $Cd25^+Gitr^{high}Nrp^+$ (upper middle panel), and $Cd25^+$ $Gitr^{high}$ $Insb^+$ cells (upper right panel) in $Cd3^+Cd4^+$ cells isolated from pancreas infiltrate and pancreatic lymph nodes and percentage of $Igrp^+$ (lower left panel), Nrp^+ (lower middle panel), and Insb $^+$(lower right panel) GITRsp cells in $Cd3^+Cd4^+$ cells isolated from pancreas infiltrate and pancreatic lymph nodes from NOD mice, 3 weeks after the graft of e/cps or G3C/cps compared with the same cells of control mice (baseline). The gating strategy is identical to that reported in Fig. 2*C*. *C*: Histological representative images of pancreatic islets in NOD mice are shown in the upper panels. The islets were considered to be intact without (w/o) insulitis (an islet that

lymph nodes of conventional and nonconventional Tregs even after months from the beginning of treatment. Moreover, a tendency of infiltration/homing of Tregs is evident in nondiabetic untreated and e/cps-treated mice, suggesting that activated Tregs play a crucial role in the prevention of diabetes in NOD mice.

DISCUSSION

In the current study, we have demonstrated that prolonged treatment with the anti-Gitr G3c mAb promotes the expansion of conventional and nonconventional Treg-cell subsets in the spleen of healthy animals and diabetes-prone NOD mice and in the pancreas of NOD mice at 3 weeks after the beginning of treatment. G3c-induced Treg-cell expansion was correlated with the prevention/delay of diabetes development in NOD mice and a decrease in the number of disrupted islets.

When we evaluated the animals at the end of the observation period (3 months after the beginning of the treatment), the number of expanded splenic Treg cells was comparable between e/cps-treated and G3C/cps-treated NOD mice. Since Nti et al. (44) demonstrated that diabetes development is associated with an increase in $Foxp3^+$ Treg cells in the spleen of NOD mice along with an almost complete disappearance of these cells in pancreatic lymph nodes, we investigated the expression levels of Foxp3, Gitr, and Cd25 in the pancreas of diabetic and healthy NOD mice at the end of the 3-month observation period or when we had to sacrifice them due to continued high levels of BG. We used for gene expression analysis pancreatic sections surrounded by small pancreatic lymph nodes present on the surface of the pancreas. Therefore, our results take into account both pancreatic-infiltrating T cells as well as T cells in pancreatic lymph nodes. Our results confirm and support the findings of Nti et al. (44), who suggested that the destruction of islets correlates with a relevant decrease of $Foxp3^+$ Treg cells in the pancreatic lymph nodes. Interestingly, in the pancreas of G3C/cps-treated NOD mice, the levels of Foxp3 and Gitr were similar to those found in untreated and e/cps-treated NOD mice that did not develop diabetes. These findings together indicate that G3c-induced Treg-cell expansion provides protection against the development of diabetes and that a high level of Treg in the pancreas protects from the development of diabetes, independently from the treatment. Accordingly, Bluestone et al. (45) performed a phase I study to treat T1D using expanded polyclonal cells, suggesting that Treg cells have the potential of treating T1D.

Data by Nti et al. (44) and our data demonstrate that Treg cells are present at low levels in the pancreas of NOD mice with diabetes, although Treg cells are present in a sufficient number in the lymphoid organs. The absence of pancreatic Treg cells may be due to a defect in the migration of these cells into the organ, death of resident Treg cells, and/or their instability in a proinflammatory microenvironment, which led them toward a Th-effector phenotype such as Th17 (46). G3c-induced Treg-cell expansion could have a stable Treg phenotype or migrate to the pancreas due to their antigen specificity. Several pieces of evidence suggest that Treg cells expressing high levels of Gitr are activated and function as memory Treg cells (19,47), as confirmed in this context (Supplementary Fig. 7). We can thus hypothesize that Gitr triggering leads to the preferential expansion of a certain type of Treg cells that tend to migrate into the pancreas because they are specific for pancreatic antigens. Indeed, antigen-specific conventional and nonconventional Tregs are expanded after Gitr triggering (Figs. 2*C* and 3*B* and Supplementary Fig. 9). The hypothesis that expanded antigen-specific Tregs migrate from the periphery to the pancreas is confirmed by the fact that the increase of antigen-specific Treg cells (in particular, $Insb^+$ cells) after G3c treatment is much more relevant in the pancreas (Fig. 3*B*) than in the spleen (Fig. 2*C*). Accordingly, Spence et al. (48) demonstrated that Tregs specific for insulin, proinsulin, and preproinsulin are present in the pancreas of NOD mice and are expanded in the islets.

The increase of some Treg subsets after GITR triggering may suggest that the treatment causes a generalized immunosuppression of the mice, even if the increase of B cells and $Cd4^+$ T cells in the spleen may suggest that it is not the case. Moreover, in SV129 mice, we observed an increase of IgG2a concentration in the serum, an Ig with stimulating properties, and in NOD mice we observed also the increase of $Cd8^+$ splenocytes. Therefore, even if the hypothesis of G3c-induced immunosuppression cannot be excluded, some data seem to suggest that Gitr triggering dictates more immunomodulation than immunosuppression. Future studies will investigate this crucial matter evaluating the response of treated animals to viruses, bacteria, and fungi.

Besides the immunosuppression issue, at least other four points should be addressed in the hypothesis of translating our findings to humans: *1*) an anti-human GITR antibody able to have the same effects of G3c must be found; *2*) it is necessary to find the optimal way to purify, stabilize, and administer the antibody, provided

shows absence of cell infiltration); intact with insulitis (an islet that is damaged–<50% of the islet area infiltrated or infiltration is restricted to the periphery of the islet); disrupted (an islet with severe intrainsulitis in which >50% of the islet area is infiltrated). Scale bars = 200 μm. e/cps- and G3C/cps-treated mice were sacrificed at 3 weeks after capsule implant. They were euglycemic. As a comparison, untreated euglycemic 8-week-old NOD mice (baseline) were evaluated. The percentage of "intact w/o insulitis," "intact with insulitis," and "disrupted" islets compared with all islet was calculated for each animal, and the mean ± SD value is reported in the lower panels. *P* values for *A* and *B* were calculated using one-way ANOVA (Tukey) or Kruskal-Wallis (Dunn) when the KS normality test failed. Nonsignificant values ($P > 0.05$) are not shown.

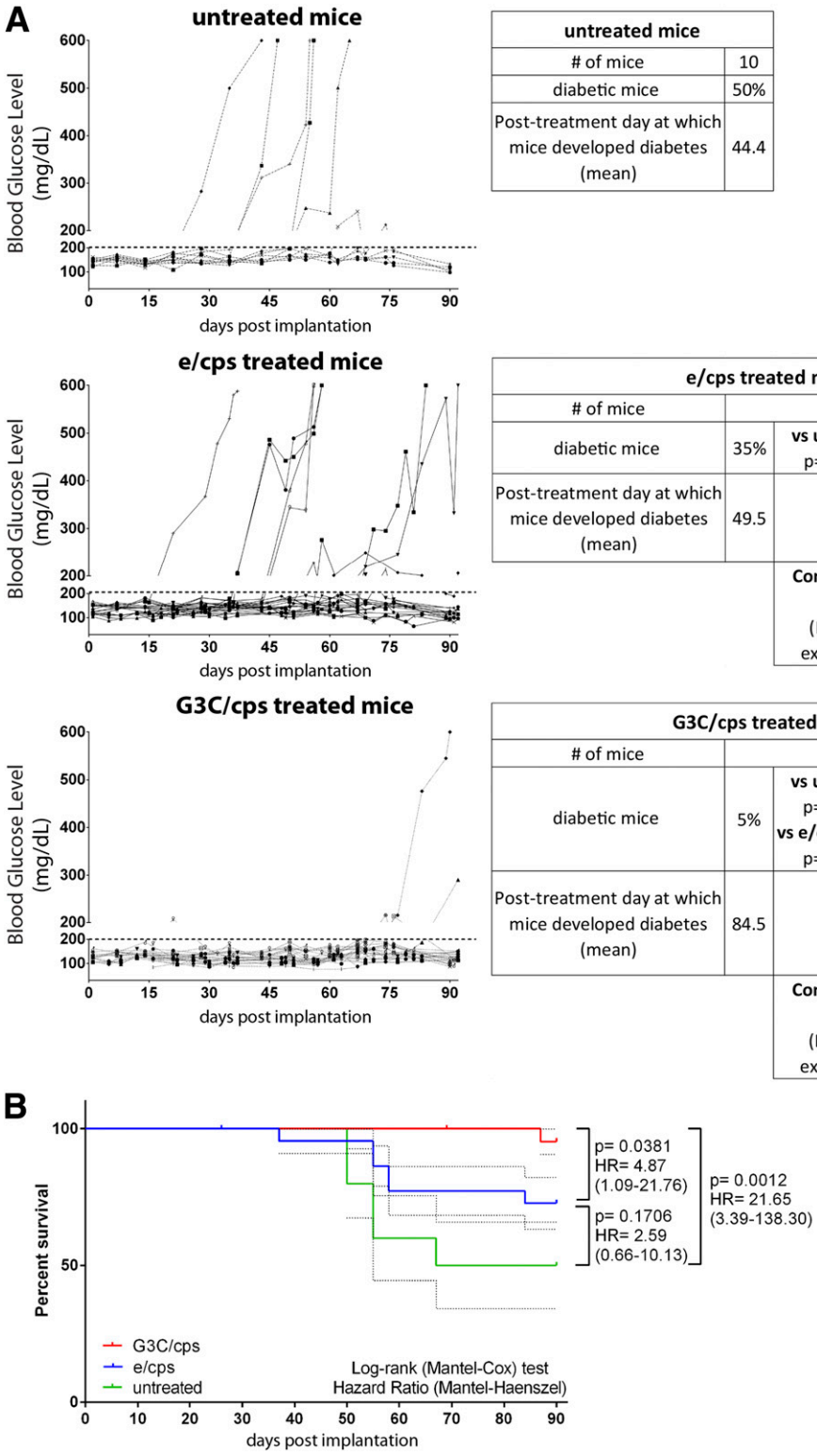

untreated mice	
# of mice	10
diabetic mice	50%
Post-treatment day at which mice developed diabetes (mean)	44.4

e/cps treated mice			
# of mice	23		
diabetic mice	35%	**vs untreated** p= 0.4611	/
Post-treatment day at which mice developed diabetes (mean)	49.5	/	**vs untreated** p= 0.5692
		Contingency test (Fisher's exact test)	**Student t-test** (unpaired t-test)

G3C/cps treated mice			
# of mice	21		
diabetic mice	5%	**vs untreated** p= 0.0075 **vs e/cps treated** p= 0.0227	/
Post-treatment day at which mice developed diabetes (mean)	84.5	/	**vs untreated** p= 0.0065 **vs e/cps treated** p= 0.0287
		Contingency test (Fisher's exact test)	**Student t-test** (unpaired t-test)

Figure 4—Lower glycemic levels and higher survival rate of G3C/cps-treated than untreated and e/cps-treated NOD mice in the long-term experiment. *A*: The BG levels of untreated (left upper panel), e/cps-treated (left middle panel), and G3C/cps-treated (left lower panel) mice are shown. Mice with a BG level higher than 500 mg/dL in two evaluations were sacrificed. Tables on the right indicate the number of mice belonging to each group, the percentage of diabetic mice at the end of the observation period, and the mean posttreatment day at which a mouse showed high BG (BG >200 mg/dL on two consecutive evaluations). Significance compared with untreated and e/cps-treated mice was calculated using the contingency test and Student *t* test as reported in the tables. *B*: Kaplan-Meier (± SEM) curves of untreated and e/cps- and G3C/cps-treated mice. The log-rank Mantel-Cox test was used for comparing survival curves. The hazard ratio (95% CI), calculated with the Mantel-Haenszel method, is shown on the right.

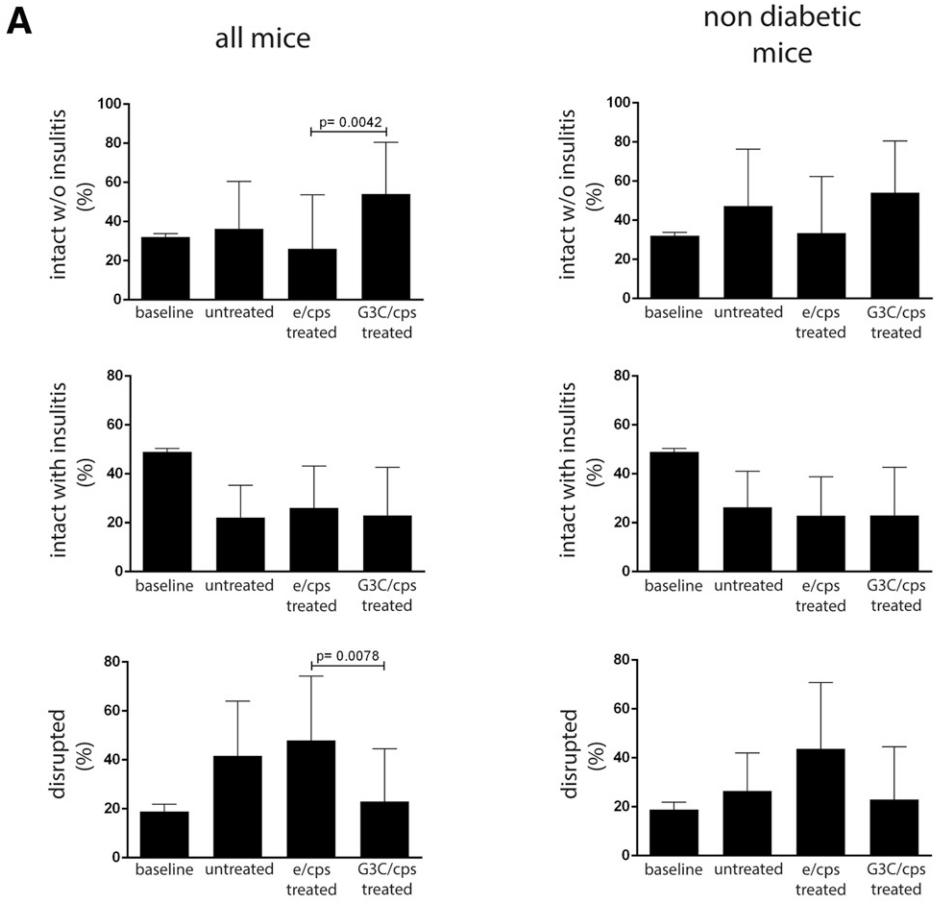

B

		all mice			
		baseline	untreated	e/cps treated	G3C/cps treated
disrupted/ intact w/o insulitis	ratio	0.59	1.15	1.84	0.42
	min - max values	0.5 - 0.68	0.005 - 6.52	0.036 - 464.00	0.0011 - 5.04

		non diabetic mice			
		baseline	untreated	e/cps treated	G3C/cps treated
disrupted/ intact w/o insulitis	ratio	0.59	0.56	1.31	0.42
	min - max values	0.5 - 0.68	0.005 - 1.50	0.036 - 198.00	0.0011 - 5.04

Figure 5—There was less pancreatic islet damage in G3C/cps-treated compared with untreated and e/cps-treated NOD mice in the long-term experiment. *A*: In the long-term experiment (Supplementary Fig. 1), the pancreas of G3C/cps-treated mice was compared with that of untreated and e/cps-treated mice. As a further control, the pancreas of untreated euglycemic NOD mice on day 0 (baseline) was evaluated. Mice were sacrificed when BG was >500 mg/dL or at the end of the observation period (3 months). The percentage of "intact without (w/o) insulitis" (upper panel), "intact with insulitis" (middle panel), and "disrupted" (lower panel) islets compared with all islets was calculated for each animal, and the mean (± SD) value of each group is reported (left panels). The percentage of "intact w/o insulitis" (upper panel), "intact with insulitis" (middle panel), and "disrupted" (lower panel) islets compared with all islets was calculated for nondiabetic animals (sacrificed at the end of the experiment), and the mean (± SD) value of each group is reported (right panels). *P* values were calculated using one-way ANOVA (Tukey) or Kruskal-Wallis (Dunn) when the KS normality test failed. Nonsignificant values ($P > 0.05$) are not shown. *B*: The mean percentage ratio of "disrupted" islets vs. "intact w/o insulitis" islets was calculated. Moreover, the mean percentage ratio of "disrupted" islets vs. "intact w/o insulitis" islets was calculated for each animal, and the minimum and maximum values are reported.

that administration of microencapsulated hybridoma cells may have a low safety profile; *3*) the best dose of the antibody must be found; and *4*) the length of the effect of the treatment has to be determined. The appearance of diabetic G3C/cps-treated mice at the end of the study may suggest that the effect of the treatment in NOD mice lasts 3–4 months. The resulting in vivo effects of Gitr triggering is dependent on the context, the disease, and the way by which Gitr is stimulated (28). The anti-Gitr DTA-1 mAb activates $Cd8^+$ T cells and promotes tumor rejection via

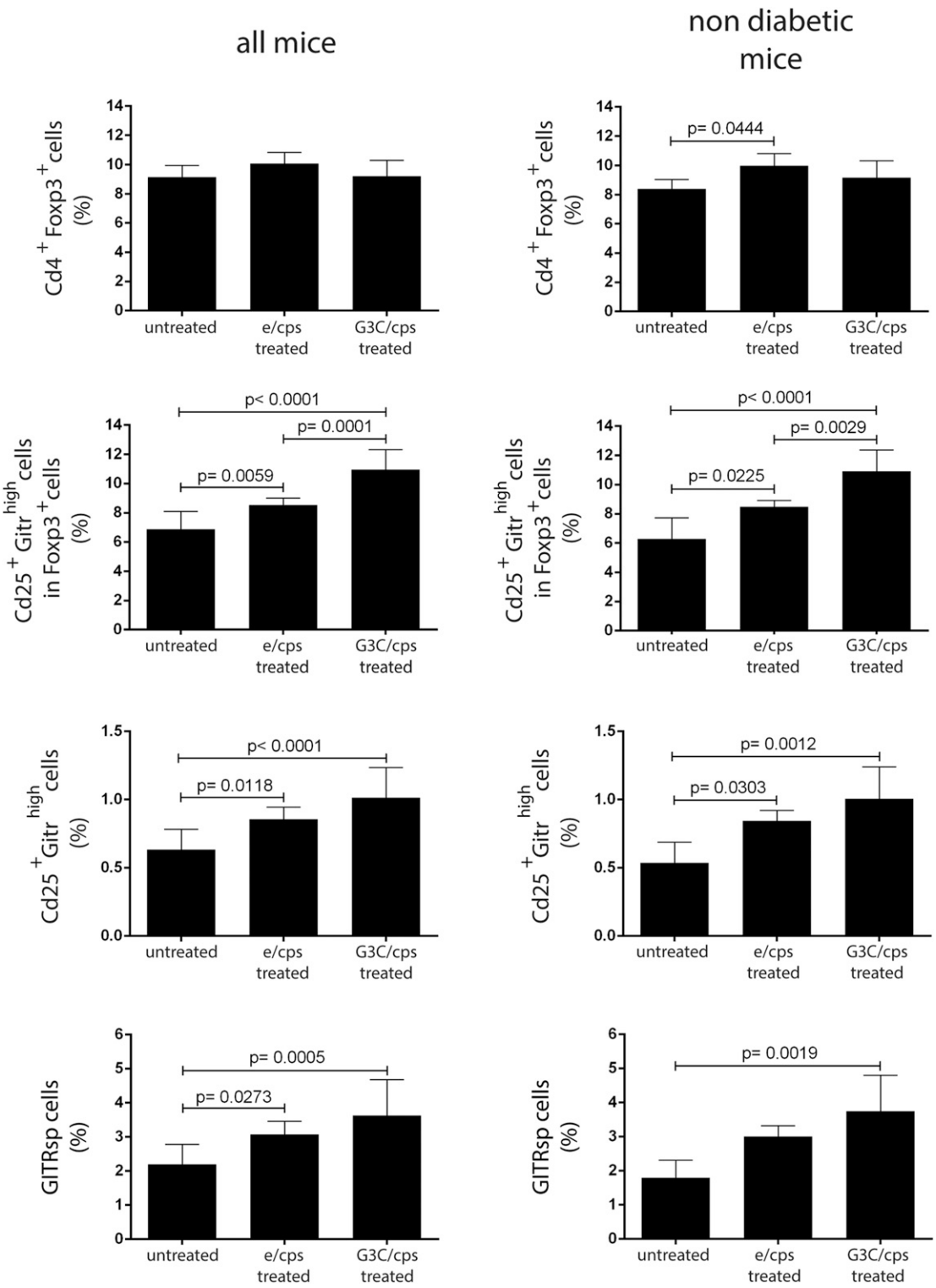

Figure 6—G3c-dependent expansion of conventional and nonconventional Treg-cell subsets in the spleens of NOD mice in the long-term experiment. Percentage of $Cd4^+Foxp3^+$ cells in $Cd3^+$ splenocytes (upper panels), of $Cd25^+Gitr^{high}$ cells in $Cd4^+Foxp3^+$ splenocytes (middle-upper panels), of $Cd4^+Foxp3^+Cd25^+Gitr^{high}$ cells in $Cd3^+$ splenocytes (middle-lower panels), and of $Cd4^+Foxp3^{-/low}Cd25^-Gitr^{int/high}$ (GITRsp) cells in $Cd3^+$ splenocytes (lower panels) from NOD mice, after the graft of e/cps or G3C/cps compared with untreated mice. The mice were sacrificed when BG was >500 mg/dL or at the end of the experiment (all the mice of the group, left panels). Data obtained only from nondiabetic mice (sacrificed at the end of the experiment) are reported in the right panels. *P* values were calculated using one-way ANOVA (Tukey) or Kruskal-Wallis (Dunn) when the KS normality test failed. Nonsignificant values ($P > 0.05$) are not shown.

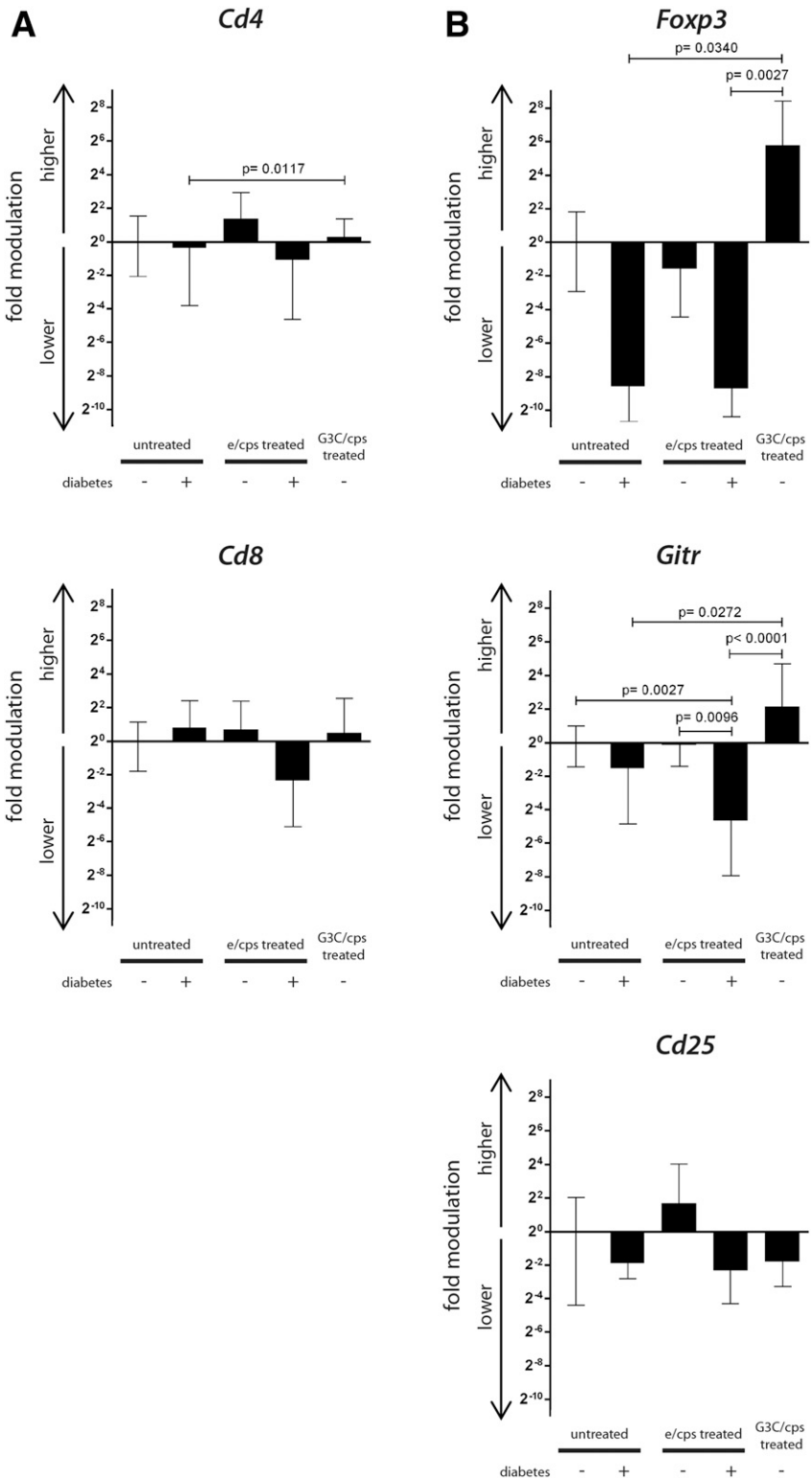

Figure 7—Expression of T- and Treg-cell markers in the pancreatic islets of G3C/cps-treated compared with untreated and e/cps-treated NOD mice in the long-term experiment. mRNA expression of T lymphocyte-cell markers in the pancreas of untreated (diabetic and nondiabetic), e/cps-treated (diabetic and nondiabetic), and G3C/cps-treated (nondiabetic) NOD mice. Mice were sacrificed only when BG was >500 mg/dL or at the end of the experiment. mRNA expression of genes was evaluated by real-time qPCR and normalized to GAPDH expression. For each pancreas, T-cell markers were further normalized to the mean expression value of the markers expressed in the pancreas of untreated nondiabetic NOD mice, which was considered to be equal to 1. For each sample, the real-time qPCR was performed twice with similar results. The mean ± SD values are shown. *P* values were calculated using one-way ANOVA (Tukey) or Kruskal-Wallis (Dunn) when the KS normality test failed. Nonsignificant values ($P > 0.05$) are not shown. mRNA expression of Cd4 and Cd8 T-cell markers (*A*) and Treg-cell markers Foxp3, Gitr, and Cd25 (*B*) are shown.

the ADCC of Treg cells only when it is administered some days after tumor implantation (18,23,24). A GitrL fusion protein containing the Fc domain that was designed to maximize valency and the potential to agonize Gitr (GitrL-Fc) has been reported to have similar effects (49). On the contrary, the anti-Gitr G3c IgM mAb and another kind of GitrL fusion protein (a pentameric GitrL extracellular domain that does not contain Fc fragments) do not promote tumor rejection because not only T cells but also Treg cells are stimulated (34,35). Despite the context-dependent and the tool-dependent effect of Gitr binding, we can assume that in the healthy mouse, the main effect of Gitr triggering is the expansion of Treg cells (19,47). This is supported by the finding that the number of Treg cells is lower in GitrL$^{-/-}$ and Gitr$^{-/-}$ mice (29–31) and higher in GitrL transgenic mice (32,33). In the presence of interleukin 2 and anti-Cd3 mAbs, Gitr activation by the GitrL-Fc fusion protein promotes the proliferation of both conventional T cells and Treg cells; however, Foxp3^{+} cells exhibit a stronger response to the ligation of Gitr than Foxp3^{-} cells (50). One of the reasons for this effect is that Gitr is expressed at the highest levels by Treg cells (47,51). Our study confirms that the effects of Gitr triggering depend on the context and the way through which Gitr is triggered. In this model, the agonist anti-Gitr G3c IgM mAb promotes more Treg-cell expansion than conventional T-cell expansion.

A recent study demonstrated that treatment of NOD mice with purified IgM reverses new-onset diabetes and enhances Treg-cell numbers (52). Therefore, it can be hypothesized that Gitr triggering and an IgM-specific effect work synergistically to prevent the development of diabetes. The more relevant of these two mechanisms needs to be investigated in future studies using purified G3c mAb and polyclonal IgM antibody. However, in the current study, the observed expansion of Gitr^{+} T cells after treatment suggests that Gitr triggering plays a determinant role in the prevention/delay of diabetes.

The current study, however, has some limitations, and the main one is the low number of NOD mice that developed diabetes after e/cps treatment. This could be the result of the surgical procedure used to implant the microcapsules in the peritoneum as well as the microencapsulation procedure itself. Moreover, our study lacks isotype control because AG microcapsules do not allow testing of polyclonal IgM antibodies; therefore, it is impossible to assess whether the IgM itself or Gitr triggering play the most relevant effect. Another limitation of our study is the length of the observation period of G3C-treated mice (3 months); thus, it is impossible to state whether the treatment prevents or delays diabetes development. In addition, it is important to account for the products released by the hybridoma that, along with the antibody, may have influenced the effects of the anti-Gitr IgM.

In conclusion, the findings of the current study showed that the treatment of NOD mice with G3c mAb microcapsules delayed/prevented diabetes and are proof of concept that support the idea that Gitr signaling can induce Treg cells in vivo, thus improving the outcome of T1D. Therefore, further treatment modalities with antibodies or fusion proteins that are able to stimulate human GITR should be tested in humanized murine models. Such biotechnological drugs that are able to trigger GITR may represent a promising therapeutic approach to inhibit diabetes development by inducing Treg-cell expansion. Induction of Treg-cell expansion in early-onset T1D, when 20−30% of islet β-cells are damaged but not completely destroyed, may enable recovery of the pancreatic β-cell fraction to a level that is sufficient to maintain fairly efficient BG levels in the absence of exogenous insulin supplementation. This therapeutic approach might be eventually successful in the early treatment of patients with newly diagnosed T1D.

Acknowledgments. We thank Yehuda Shoenfeld of Tel-Aviv University, Tel-Aviv, Israel, and the Zabludovicz Center for Autoimmune Diseases, The Chaim Sheba Medical Center, Tel-Hashomer, Israel, for taking some time to share his knowledge with us a few years ago. This gave us the confidence to pursue our research project and demonstrate the clinical usefulness of GITR triggering in treating autoimmune diseases.

Funding. G.N. was supported by Fondo di Ateneo per la ricerca di base 2015. C.R. was supported by the Ministero dell'Istruzione, dell'Università e della Ricerca (MIUR) under grant number 2015ZT9MXY_001.

Duality of Interest. G.N. is a consultant for Pieris Pharmaceuticals, Inc. No other potential conflicts of interest relevant to this article were reported.

Author Contributions. L.C. set up and performed ELISA experiments. L.C. created the figures. L.C. performed immune characterization of WT, Gitr$^{-/-}$, and NOD mice, including flow cytometry, proliferation experiments, and qPCR, with the help of M.G.P. and E.R. L.C. and G.N. analyzed cytofluorimetric data. P.M. and G.B. conducted the histological analysis on islets. P.M., G.B., T.P., and A.G. microencapsulated the hybridoma. P.M., T.P., and A.G. monitored NOD mice, evaluating glycemia. G.B. and S.C. grafted microcapsules in WT, Gitr$^{-/-}$, and NOD mice. M.G.P. and E.R. studied the best growth conditions for G3C hybridoma. M.G.P., J.S., G.M., R.C., and C.R. contributed to writing the manuscript. J.S. developed G3C hybridoma. G.M, R.C., and C.R. contributed to conception and supervision of the project. G.N. conceived and supervised the project. G.N. wrote the manuscript. G.N. is the guarantor of this work and, as such, had full access to all the data in the study and takes responsibility for the integrity of the data and the accuracy of the data analysis.

Prior Presentation. Data from this study were presented at the 78th Scientific Sessions of the American Diabetes Association, Orlando, FL, 22–26 June 2018; IPITA (International Pancreas and Islet Transplant Association) 2017 – 16th International Congress, Oxford, U.K., 20–23 June 2017; and the 8th International Conference on Autoimmunity: Mechanisms and Novel Treatments, Rhodes, Greece, 17–22 September 2017.

References

1. Atkinson MA, Eisenbarth GS, Michels AW. Type 1 diabetes. Lancet 2014;383:69–82
2. Sherwin R, Jastreboff AM. Year in diabetes 2012: the diabetes tsunami. J Clin Endocrinol Metab 2012;97:4293–4301
3. Noble JA. Immunogenetics of type 1 diabetes: a comprehensive review. J Autoimmun 2015;64:101–112
4. Babon JAB, DeNicola ME, Blodgett DM, et al. Analysis of self-antigen specificity of islet-infiltrating T cells from human donors with type 1 diabetes. Nat Med 2016;22:1482–1487
5. Ziegler AG, Rewers M, Simell O, et al. Seroconversion to multiple islet autoantibodies and risk of progression to diabetes in children. JAMA 2013;309:2473–2479
6. Sherry NA, Chen W, Kushner JA, et al. Exendin-4 improves reversal of diabetes in NOD mice treated with anti-CD3 monoclonal antibody by enhancing recovery of β-cells. Endocrinology 2007;148:5136–5144

7. Ogawa N, List JF, Habener JF, Maki T. Cure of overt diabetes in NOD mice by transient treatment with anti-lymphocyte serum and exendin-4. Diabetes 2004; 53:1700–1705
8. Suri A, Calderon B, Esparza TJ, Frederick K, Bittner P, Unanue ER. Immunological reversal of autoimmune diabetes without hematopoietic replacement of beta cells. Science 2006;311:1778–1780
9. Weir GC, Bonner-Weir S. Dreams for type 1 diabetes: shutting off autoimmunity and stimulating beta-cell regeneration. Endocrinology 2010;151:2971–2973
10. Alipio Z, Liao W, Roemer EJ, et al. Reversal of hyperglycemia in diabetic mouse models using induced-pluripotent stem (iPS)-derived pancreatic beta-like cells. Proc Natl Acad Sci U S A 2010;107:13426–13431
11. Tsai S, Shameli A, Yamanouchi J, et al. Reversal of autoimmunity by boosting memory-like autoregulatory T cells. Immunity 2010;32:568–580
12. Chatenoud L, Thervet E, Primo J, Bach JF. Anti-CD3 antibody induces long-term remission of overt autoimmunity in nonobese diabetic mice. Proc Natl Acad Sci U S A 1994;91:123–127
13. Kroger CJ, Clark M, Ke Q, Tisch RM. Therapies to suppress β cell autoimmunity in type 1 diabetes. Front Immunol 2018;9:1891
14. Bluestone JA, Tang Q. T_{reg} cells-the next frontier of cell therapy. Science 2018;362:154–155
15. Weber SE, Harbertson J, Godebu E, et al. Adaptive islet-specific regulatory CD4 T cells control autoimmune diabetes and mediate the disappearance of pathogenic Th1 cells in vivo. J Immunol 2006;176:4730–4739
16. Gagliani N, Jofra T, Stabilini A, et al. Antigen-specific dependence of Tr1-cell therapy in preclinical models of islet transplant. Diabetes 2010;59:433–439
17. Nocentini G, Cari L, Migliorati G, Riccardi C. Treatment of autoimmune diseases and prevention of transplant rejection and graft-versus-host disease by regulatory T cells: the state of the art and perspectives. In *The Epigenetics of Autoimmunity: (Translational Epigenetics; vol. 5)*. Zhang R, Ed. San Diego, Academic Press, 2018, p. 321–357
18. Riccardi C, Ronchetti S, Nocentini G. Glucocorticoid-induced TNFR-related gene (GITR) as a therapeutic target for immunotherapy. Expert Opin Ther Targets 2018;22:783–797
19. Ronchetti S, Ricci E, Petrillo MG, et al. Glucocorticoid-induced tumour necrosis factor receptor-related protein: a key marker of functional regulatory T cells. J Immunol Res 2015;2015:171520
20. Cari L, Nocentini G, Migliorati G, Riccardi C. Potential effect of tumor-specific Treg-targeted antibodies in the treatment of human cancers: a bioinformatics analysis. OncoImmunology 2017;7:e1387705
21. Padovani CTJ, Bonin CM, Tozetti IA, Ferreira AMT, dos Santos Fernandes CE, Costa IP. Glucocorticoid-induced tumor necrosis factor receptor expression in patients with cervical human papillomavirus infection. Rev Soc Bras Med Trop 2013;46:288–292
22. Wang M-X, Ren J-T, Tang L-Y, Ren Z-F. Molecular features in young vs elderly breast cancer patients and the impacts on survival disparities by age at diagnosis. Cancer Med 2018;7:3269–3277
23. Ko K, Yamazaki S, Nakamura K, et al. Treatment of advanced tumors with agonistic anti-GITR mAb and its effects on tumor-infiltrating Foxp3+CD25+CD4+ regulatory T cells. J Exp Med 2005;202:885–891
24. Bulliard Y, Jolicoeur R, Windman M, et al. Activating Fc γ receptors contribute to the antitumor activities of immunoregulatory receptor-targeting antibodies. J Exp Med 2013;210:1685–1693
25. Ono M, Shimizu J, Miyachi Y, Sakaguchi S. Control of autoimmune myocarditis and multiorgan inflammation by glucocorticoid-induced TNF receptor family-related protein(high), Foxp3-expressing CD25+ and CD25- regulatory T cells. J Immunol 2006;176:4748–4756
26. Alunno A, Petrillo MG, Nocentini G, et al. Characterization of a new regulatory CD4+ T cell subset in primary Sjögren's syndrome. Rheumatology (Oxford) 2013;52:1387–1396
27. Nocentini G, Alunno A, Petrillo MG, et al. Expansion of regulatory GITR+CD25 low/-CD4+ T cells in systemic lupus erythematosus patients. Arthritis Res Ther 2014;16:444
28. Ephrem A, Epstein AL, Stephens GL, Thornton AM, Glass D, Shevach EM. Modulation of Treg cells/T effector function by GITR signaling is context-dependent. Eur J Immunol 2013;43:2421–2429
29. Nocentini G, Ronchetti S, Cuzzocrea S, Riccardi C. GITR/GITRL: more than an effector T cell co-stimulatory system. Eur J Immunol 2007;37:1165–1169
30. Ronchetti S, Nocentini G, Riccardi C, Pandolfi PP. Role of GITR in activation response of T lymphocytes. Blood 2002;100:350–352
31. Stephens GL, McHugh RS, Whitters MJ, et al. Engagement of glucocorticoid-induced TNFR family-related receptor on effector T cells by its ligand mediates resistance to suppression by CD4+CD25+ T cells. J Immunol 2004;173:5008–5020
32. van Olffen RW, Koning N, van Gisbergen KPJM, et al. GITR triggering induces expansion of both effector and regulatory CD4+ T cells in vivo. J Immunol 2009; 182:7490–7500
33. Carrier Y, Whitters MJ, Miyashiro JS, et al. Enhanced GITR/GITRL interactions augment IL-27 expression and induce IL-10-producing Tr-1 like cells. Eur J Immunol 2012;42:1393–1404
34. Nishioka T, Nishida E, Iida R, Morita A, Shimizu J. In vivo expansion of CD4+ Foxp3+ regulatory T cells mediated by GITR molecules. Immunol Lett 2008;121:97–104
35. Kim YH, Shin SM, Choi BK, et al. Authentic GITR signaling fails to induce tumor regression unless Foxp3+ regulatory T cells are depleted. J Immunol 2015; 195:4721–4729
36. Montanucci P, Cari L, Basta G, et al. Engineered alginate microcapsules for molecular therapy through biologic secreting cells. Tissue Eng Part C Methods 2019;25:296–304
37. Fallarino F, Luca G, Calvitti M, et al. Therapy of experimental type 1 diabetes by isolated Sertoli cell xenografts alone. J Exp Med 2009;206:2511–2526
38. Cari L, Ricci E, Gentili M, et al. A focused real time PCR strategy to determine GILZ expression in mouse tissues. Results Immunol 2015;5:37–42
39. Calafiore R, Basta G, Luca G, et al. Standard technical procedures for microencapsulation of human islets for graft into nonimmunosuppressed patients with type 1 diabetes mellitus. Transplant Proc 2006;38:1156–1157
40. Basta G, Montanucci P, Luca G, et al. Long-term metabolic and immunological follow-up of nonimmunosuppressed patients with type 1 diabetes treated with microencapsulated islet allografts: four cases. Diabetes Care 2011;34:2406–2409
41. Gasperini L, Mano JF, Reis RL. Natural polymers for the microencapsulation of cells. J R Soc Interface 2014;11:20140817
42. Nocentini G, Cari L, Migliorati G, Riccardi C. The role of GITR single-positive cells in immune homeostasis. Immun Inflamm Dis 2017;5:4–6
43. Bianchini R, Bistoni O, Alunno A, et al. CD4(+) CD25(low) GITR(+) cells: a novel human CD4(+) T-cell population with regulatory activity. Eur J Immunol 2011;41:2269–2278
44. Nti BK, Markman JL, Bertera S, et al. Treg cells in pancreatic lymph nodes: the possible role in diabetogenesis and β cell regeneration in a T1D model. Cell Mol Immunol 2012;9:455–463
45. Bluestone JA, Buckner JH, Fitch M, et al. Type 1 diabetes immunotherapy using polyclonal regulatory T cells. Sci Transl Med 2015;7:315ra189
46. Betto E, Usuelli V, Mandelli A, et al. Mast cells contribute to autoimmune diabetes by releasing interleukin-6 and failing to acquire a tolerogenic IL-10$^+$ phenotype. Clin Immunol 2017;178:29–38
47. Petrillo MG, Ronchetti S, Ricci E, et al. GITR+ regulatory T cells in the treatment of autoimmune diseases. Autoimmun Rev 2015;14:117–126
48. Spence A, Purtha W, Tam J, et al. Revealing the specificity of regulatory T cells in murine autoimmune diabetes. Proc Natl Acad Sci U S A 2018;115:5265–5270
49. Leyland R, Watkins A, Mulgrew KA, et al. A novel murine GITR ligand fusion protein induces antitumor activity as a monotherapy that is further enhanced in combination with an OX40 agonist. Clin Cancer Res 2017;23:3416–3427
50. Liao G, Nayak S, Regueiro JR, et al. GITR engagement preferentially enhances proliferation of functionally competent CD4+CD25+FoxP3+ regulatory T cells. Int Immunol 2010;22:259–270
51. Shimizu J, Yamazaki S, Takahashi T, Ishida Y, Sakaguchi S. Stimulation of CD25(+)CD4(+) regulatory T cells through GITR breaks immunological self-tolerance. Nat Immunol 2002;3:135–142
52. Wilson CS, Chhabra P, Marshall AF, et al. Healthy donor polyclonal IgMs diminish B-lymphocyte autoreactivity, enhance regulatory T-cell generation, and reverse type 1 diabetes in NOD mice. Diabetes 2018;67:2349–2360